Hydrogen Bonding and Intermolecular Vibrations of 6-Hydroxyquinoline·H_2O in the S_0 and S_1 States

Andreas Bach, Johannes Hewel, and Samuel Leutwyler*

Departement für Chemie und Biochemie, Universität Bern, Freiestrasse 3, CH-3000 Bern 9, Switzerland

Received: June 22, 1998; In Final Form: September 23, 1998

A combined spectroscopic and ab initio theoretical study of the hydrogen-bonded 6-hydroxyquinoline·H_2O complex was performed. 6-Hydroxyquinoline (6-HQ) is bifunctional, acting as an H-bond donor at the O−H group and as an acceptor at the N atom in bulk aqueous solution. Excited-state proton transfer (ESPT) from 6-HQ to the solvent occurs adiabatically in the S_1 state, involving proton transfer at both functional groups. We have measured the mass- and rotamer-resolved $S_1 \leftarrow S_0$ vibronic spectra of cis- and trans rotamers of 6-HQ and of both the *cis*- and *trans*-6-HQ·H_2O complexes in supersonic jets, using two-color resonant two-photon ionization spectroscopy and UV/UV spectral hole-burning techniques. Following the identification of the cis and trans rotamer electronic origins, dispersed fluorescence emission spectra of both rotamers of 6-HQ and 6-HQ·H_2O were measured. The results are consistent with H_2O bonded exclusively to the hydroxyl group and not to the N atom. Equilibrium structures were calculated by ab initio SCF methods for both rotamers of 6-HQ and both the *cis*- and *trans*-6-HQ·H_2O complexes and give C_s symmetric structures with trans-linear hydrogen bonds. The calculated torsional transition states for H atom exchange on the H_2O subunit are nonplanar with C_1 symmetry. The calculated H-bond dissociation energies are ≈ 5.9 kcal/mol for the cis and ≈ 6.0 kcal/mol trans rotamer, slightly stronger than those of 2-naphthol·H_2O (5.8 kcal/mol) and phenol·H_2O (5.6 kcal/mol). Harmonic normal-mode frequencies allow detailed assignments of the observed inter- and intramolecular vibronic transitions. Agreement between theory and experiment is generally good, with the exception of the β_2 wag mode.

1. Introduction

6-Hydroxyquinoline (6-HQ) is a bifunctional hydrogen-bonding molecule, which in aqueous or alcoholic solution simultaneously acts as a H-bond donor at the O−H group and as an acceptor at the N atom. Electronic excitation to the S_1 state strongly modifies the acid−base properties of this molecule at both positions, rendering the hydroxyl group more acidic and the N atom more basic. As a consequence, S_1 excited-state proton transfer (ESPT) from 6-HQ to the solvent occurs adiabatically in bulk water and also other protic solvents.[1−3] Valeur et al.[3] have recently undertaken a comprehensive study of the prototropic equilibria and kinetics of 6-HQ in acidic, basic, and neutral aqueous solutions and have confirmed the extremely high simultaneous photoacidity and photobasicity in the S_1, excited state, where deprotonation can occur in 10 M $HClO_4$ and protonation in 12 M NaOH!

ESPT to bulk room-temperature solvents has also been extensively investigated for the related 7-hydroxyquinoline molecule, both by steady-state[1,4−6] and by picosecond measurements,[7−10] and also in low-temperature matrices.[5] Various models have been put forth for solvent-assisted excited-state proton transfer, i.e, a proton relay or shuttle between the −O−H group and the N atom, mediated by several solvent molecules. This possibility of solvent-mediated proton relay in small water clusters of 7-hydroxyquinoline was investigated by Lahmani et al. by laser fluorescence spectroscopy in supersonic jets.[11] These authors did *not* find evidence for a solvent-assisted excited-state proton transfer or tautomerization reactions in small water clusters, although they observed an unusually large spectral shift for a spectrum they assigned to the 7-hydroxyquinoline·$(H_2O)_3$ complex.

On the basis of its structural and electronic similarities to 1- and 2-naphthol[12] (1-HN, 2-HN), we expect jet-cooled 6-hydroxyquinoline microsolvent clusters with water and ammonia to also undergo ESPT and provide finite model systems for proton transfer.[13−20] This motivated us to investigate the supersonically cooled hydrogen-bonded 6-hydroxyquinoline·H_2O complex, using vibrationally resolved resonant two-photon ionization, UV/UV hole-burning and high-resolution dispersed fluorescence emission spectroscopy. In 6-hydroxyquinoline the acidic (H-bond-donating) and basic (H-bond-accepting) parts of the molecule are both relatively far removed from each other, ≈10 Å. Thus, a single solvent molecule cannot bind to both sites simultaneously, as is possible in, e.g., the analogous 2-hydroxypyridine·H_2O[21−24] complex. Thus, the two hydrogen-bonding sites are in competition, and it is interesting to inquire whether one site is energetically preferred, and by how much. Also, comparisons can be made with the closely related 1-naphthol and 2-naphthol complexes with H_2O and D_2O.[15,25]

We complemented the spectroscopic measurements by ab initio calculations, which give minimum-energy structures, normal-mode eigenvectors, and harmonic frequencies, cf. section II. The latter can be compared to the experimental frequencies. The internal rotation barrier of the H_2O moiety relative to the quinoline molecule was also investigated, since the large-amplitude torsional motion has recently been intensively studied for the related hydrogen-bonded complexes phenol·H_2O[26−30] and 2-naphthol·H_2O[25] and 1-naphthol·H_2O.[31]

10.1021/jp982703x CCC: $15.00
Published on Web 12/01/1998

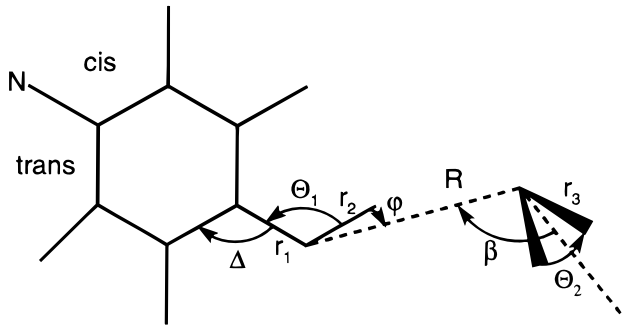

Figure 1. Definition of structural parameters for *cis*- and *trans* 6-hydroxyquinoline·H_2O. The second aromatic ring is at the positions indicated.

2. Theoretical Methods and Results

2.1. Computational Procedure. Minimum-energy structures for the *trans*- and *cis*-6-HQ rotamers, see Figure 1, and the corresponding *trans*- and *cis*-6-HQ·H_2O complexes were calculated at the SCF level using the 6-31G(d,p) basis set. To obtain highly accurate electronic energies, the convergence criteria of the self-consistent field (SCF) step were increased: the root-mean-square (RMS) difference between the density matrix elements in consecutive cycles of the procedure was required to be $<1 \times 10^{-10}$. Both inter- and intramolecular degrees of freedom were fully optimized without symmetry restrictions and converged until the largest component of the nuclear gradient was 2×10^{-6} hartree/bohr or hartree/rad.

The starting configurations were derived from the corresponding 2-HN·H_2O geometries.[25] Normal coordinate calculations were carried out at the minimum-energy geometries. The resulting *intra*molecular vibrational frequencies were scaled by a factor of 0.92 in order to account for the well-known overestimate of vibrational frequencies at the SCF level. Intermolecular vibrational frequencies remained unscaled, since there is no analogous problem on extending intermolecular bonds between closed-shell systems to the dissociation limit. The transition structures (TS) along the H-atom exchange path on the water molecule (corresponding to the intermolecular torsional vibration) were obtained for both rotamers of 6-HQ·H_2O, as well as for the trans → cis isomerization of 6-HQ by full optimization to first-order saddle points using analytical second derivatives. All ab initio calculations were performed using the GAUSSIAN 94 program.[32]

2.2. Calculated Equilibrium and Transition Structures and Binding Energies. Experimentally, one finds that 6-HQ exists both as a trans and cis rotamer, cf. Figure 1, differing in the orientation of the O−H bond with respect to the quinoline frame (see below). Comparing the calculated total energies of the corresponding optimized minimum-energy structures at the SCF 6-31G(d,p) level in the S_0 electronic ground state, the cis rotamer is predicted to be stabilized by 279 cm^{-1} relative to the trans rotamer. Including zero-point energy (ZPE) corrections, this difference is slightly lowered to 230 cm^{-1}. For the analogous 2-naphthol (2-HN) molecule,[25] the cis rotamer is also calculated to be more stable than the trans rotamer, by a similar amount of 301 cm^{-1}. The calculated electronic barrier height for the torsional trans → cis isomerization path in the S_0 electronic ground state obtained from the transition structure optimization was 740.3 cm^{-1} at the SCF 6-31G(d,p) level. Including the ZPE corrections for the $3N - 7$ nontorsional modes reduced the barrier slightly to 732.8 cm^{-1}.

For both the cis and trans rotamers, the hydrogen-bonding arrangement is closely trans-linear, with the plane of the water molecule lying perpendicular to that of the aromatic ring system. A number of structural parameters characterizing the hydrogen-bond arrangement are defined in Figure 1, and their values are compiled in Table 1. The structure parameters are very similar for the cis and trans rotamers: the interoxygen distance R(O···O) is 2.90 Å, and marginally shorter for the cis form. The only important difference is the inclination angle β between the bisector of the water molecule and the O···O line, which is smaller (i.e., more bent) for the cis form.

TABLE 1: Calculated Values of Structural Parameters of the *cis*- and *trans*-6-HQ·H_2O Complexes; cf. Figure 1 for Definitions[a]

	t-6-HQ·H_2O	*t*-6-HQ·H_2O TS	*t*-6-HQ	*c*-6-HQ·H_2O	*c*-6-HQ·H_2O TS	*c*-6-HQ
r_1 (Å)	1.344	1.343	1.353	1.343	1.341	1.351
r_2 (Å)	0.949	0.949	0.957	0.950	0.950	0.941
R (Å)	2.898	2.900		2.897	2.897	
r_3 (Å)	0.944	0.943	0.943	0.944	0.944	0.943
Θ_1 (deg)	111.90	112.06	111.43	111.58	111.91	111.18
Δ (deg)	120.89	119.15	120.42	115.93	115.91	120.89
φ (deg)	2.67	3.88		2.54	8.76	
β (deg)	132.68	144.56		132.30	143.66	
Θ_2 (deg)	106.88	106.75	105.97	106.85	106.75	105.97

[a] All values at the SCF 6-31G(d,p) level.

The calculated hydrogen-bond binding energies are 5.934 kcal/mol for the *cis*- and 6.075 kcal/mol for the *trans*-6-HQ·H_2O complex, respectively. These values are slightly larger than those calculated for the 2-naphthol·H_2O complex (5.8 kcal/mol) and phenol·H_2O (5.6 kcal/mol) at the same level of theory.

The calculation of hydrogen-bond energies at the "raw" SCF level is known to suffer from three deficiencies: (i) the finite basis-set size, (ii) the lack of inclusion of electronic correlation, and (iii) the basis set superposition error, see, e.g., ref 26. Here the basis set size cannot be easily extended, owing to the large size of the system, which needs 225 basis functions even with the 6-31G(d,p) basis. Furthermore, the theoretically predicted structure of the phenol·H_2O complex at the SCF/6-311++G(d,p) level[26] is in *poorer* agreement with experiment[33,34] than the SCF/6-31G(d,p) structure.[26] Also, for phenol·H_2O, the three deficiencies i−iii have been found to compensate each other to a large extent, as proposed by Schütz et al.,[26] and confirmed by Feller and Feyereisen[35] in a careful study using much larger basis sets and including correlation energy at the MP2 level. Finally, we note that recent accurate experimental measurements of the hydrogen-bond *dissociation* energies D_0 for 1-naphthol·H_2O and 1-naphthol·D_2O complexes agree with the calculated raw 6-31G(d,p) dissociation energy D_0 to within 100 cm^{-1} or $< 5\%$.[36]

2.3. Torsional Transition Structures and Barrier Heights. The lowest-energy transition state structures for *cis*- and *trans*-6-HQ·H_2O were also calculated. These are saddle points (Hessian index 1) on the intermolecular PES and represent the barriers for hydrogen atom exchange by torsion of the H_2O subunit. The motion along the minimum-energy path is actually a combination of torsion by 180° around the hydrogen bond and a simultaneous change in the inclination angle β from β_0 to $360° - \beta_0$. The SCF 6-31G(d,p) transition structures are nonplanar, with the H_2O moiety rotated by ≈95° and ≈86° for *cis*- and *trans*-6-HQ·H_2O, respectively, and the water oxygen atom 0.35 Å above the aromatic plane, quite similar to 2-HN·H_2O.[25] The calculated torsional barrier heights are required for a quantum-mechanical treatment of the torsional level structure, cf. section 2.5.

The purely electronic energy difference between the nonplanar transition structures and the corresponding minimum-energy

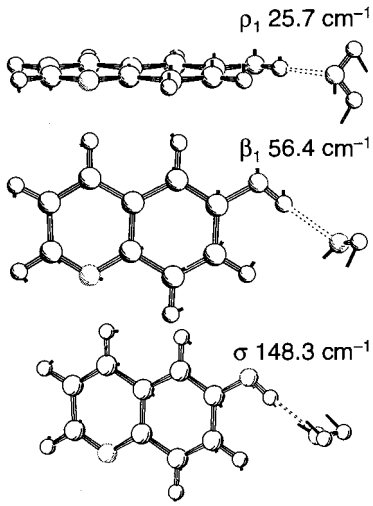

Figure 2. Perspective plots of the intermolecular normal vibrations of translational parentage of *trans*-6-HQ·H_2O with the corresponding harmonic frequencies.

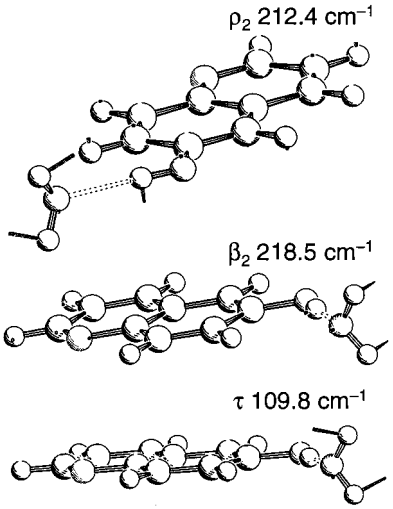

Figure 3. Perspective plot of the intermolecular normal vibrations of rotational parentage of *trans*-6-HQ·H_2O with the corresponding harmonic frequencies.

structures are 297 cm^{-1} for *cis*-6-HQ·H_2O and 287 cm^{-1} for *trans*-6-HQ·H_2O. These values are similar to the analogous barrier heights obtained for 2-HN·H_2O,[25] which are 247 cm^{-1} for the cis and 293 cm^{-1} for the trans rotamer. Inclusion of the ZPE corrections for the other $3N - 7$ modes (except the torsional mode) yields the vibrationally adiabatic barrier heights of 240 cm^{-1} for the cis and 233 cm^{-1} for the trans rotamer. The analogous values for 2-HN·H_2O are 218 cm^{-1} for the cis and 236 cm^{-1} for the trans rotamer.[25]

2.4. Intermolecular Vibrations. Six low-frequency intermolecular modes occur in the 6-HQ·H_2O complexes: the bending mode β_1, the rocking mode ρ_1, and the H-bond stretch mode σ originate from the three translational degrees of freedom of the water molecule, while the high-frequency bend mode β_2, the high-frequency rock mode ρ_2, and the torsional mode around the H-bond axis τ correlate with the three rotations of the free water molecule. σ, β_1, and β_2 are a' in-plane vibrations, whereas ρ_1, ρ_2, and τ are a'' out-of-plane modes.

The intermolecular normal-mode eigenvectors of *trans*-6-HQ·H_2O are shown in perspective views in Figures 2 and 3 together with the corresponding harmonic frequencies (unscaled). The corresponding eigenvectors for the cis rotamer are very similar and not given here. The calculated SCF 6-31G(d,p) harmonic

TABLE 2: Calculated Harmonic Frequencies, Force Constants, and Reduced Masses of the *trans*-6-HQ·H_2O Complex at the SCF Level for the 6-31G(d,p) Basis Set

irrep	label	harmonic frequency[a] (cm^{-1})	force constant ($N\ m^{-1}$)	reduced mass (amu)
a″	ρ_1	25.7	0.15	3.92
a′	β_1	56.4	0.78	4.15
a″	τ	109.8	0.77	1.08
a″	ν_1	128.6[a]	5.96	5.18
a′	σ	148.3	6.56	5.06
a″	ν_3	182.9[a]	7.68	3.3
a″	ρ_2	212.4	3.20	1.20
a′	β_2	218.5	3.69	1.31
a′	ν_4	313.1[a]	35.26	5.16
a′	ν_7	431.8[a]	97.80	7.53
a′	ν_8	469.8[a]	75.77	4.92
a′	ν_{10}	544.9[a]	123.48	5.97
a′	ν_{12}	617.0[a]	197.97	7.45
a′	ν_{14}	728.2[a]	245.67	6.65

[a] Intramolecular frequencies, scaled with 0.920, intermolecular frequencies unscaled.

TABLE 3: Calculated Harmonic Frequencies, Force Constants, and Reduced Masses of the *cis*-6-HQ·H_2O Complex at the SCF Level for the 6-31G(d,p) Basis Set

irrep	label	harmonic frequency[a] (cm^{-1})	force constant ($N\ m^{-1}$)	reduced mass (amu)
a″	ρ_1	30.9	0.20	3.52
a′	β_1	50.1	0.64	4.30
a″	τ	110.8	0.79	1.10
a″	ν_1	128.4[a]	5.79	5.04
a′	σ	152.5	7.40	5.39
a″	ν_3	181.6[a]	8.07	3.51
a′	β_2	225.9	3.85	1.28
a″	ρ_2	232.0	3.80	1.20
a′	ν_4	314.5[a]	34.37	4.99
a′	ν_7	433.5[a]	85.34	6.52
a′	ν_8	468.0[a]	83.63	5.48
a′	ν_{10}	542.6[a]	125.00	6.09
a′	ν_{12}	617.9[a]	196.52	7.39
a′	ν_{14}	731.3[a]	245.66	6.60

[a] Intramolecular frequencies, scaled with 0.920, intermolecular frequencies unscaled.

frequencies, force constants, and reduced masses of the intermolecular modes of *trans*-6-HQ·H_2O are collected in Table 2, and for the cis rotamer in Table 3.

The intermolecular modes are fairly well localized on the H_2O moiety. The low-frequency ρ_1 and β_1 modes also have noticeable motional components of the 6-HQ frame, which correspond to rigid-frame translation and/or rotation. However, the ρ_2 rocking mode involves a considerable intramolecular O−H torsional contribution on 6-HQ, and the β_2 wag mode involves a noticeable O−H in-plane bend relative to the HQ frame.

As in 2-HN·H_2O,[25] two *intramolecular* a'' modes labeled ν_1 and ν_3 fall within the intermolecular frequency range at 128/128 cm^{-1} (ν_1) and 183/182 cm^{-1} (ν_3) for the trans and cis rotamer, respectively. These two low-frequency intramolecular modes can couple with the out-of-plane motions of the water molecule, mainly ρ_1 and ρ_2.

2.5. Anharmonic Calculation of the τ Torsional Vibration in a Periodic Potential. The torsional mode has a very low reduced mass and large associated RMS vibrational amplitude; combined with the relatively low torsional barrier, the harmonic approximation is expected to be especially poor for this vibration. For an improved calculation of the torsional level structure, we applied a one-dimensional (1D) anharmonic approach, assuming approximate separability of the vibrational

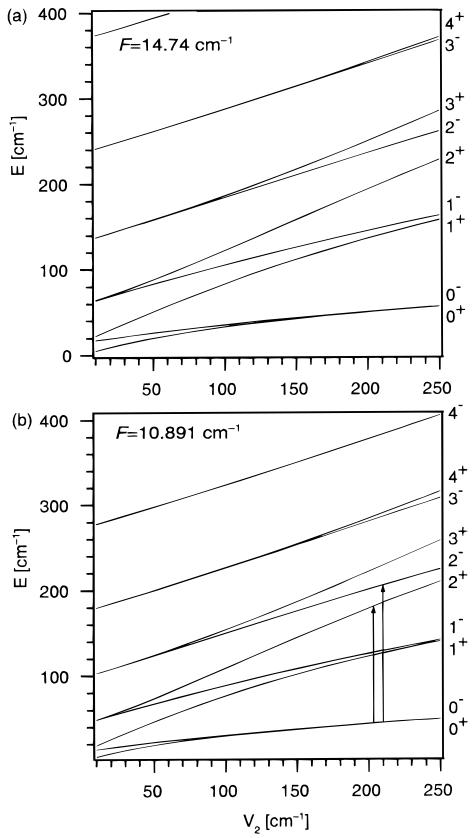

Figure 4. Vibrational level diagram for the intermolecular torsion τ as a function of the 2-fold barrier height V_2 for (a) F =14.74 and (b) F =10.89 cm^{-1}. Indicated for an estimated barrier of 213 cm^{-1} are the two optically allowed transitions $\nu = 2^+ \leftarrow \nu = 0^+$ and $\nu = 2^- \leftarrow \nu = 0^-$.

Hamiltonian in normal coordinates. This approximate separability works quite well for phenol·H_2O (refs 26, 33, 34) and 2-HN·H_2O (ref 25), as has been confirmed by the recent results of the Neusser and Kleinermanns groups.[27,28] Thus, we approximated the 1D potential energy function along the torsional τ coordinate by the a truncated Fourier series $V = V_2(1 - \cos 2\tau)/2$, where V_2 denotes the torsional barrier height and τ the angular displacement from equilibrium along τ. The next higher $V_4(1 - \cos 4\tau)/2$ term in the potential is probably small.

For the kinetic energy part, the reduced internal rotational constant F_{red} of 6-HQ·H_2O was taken to be F = 14.74 cm^{-1}, the same value as for 2-HN·H_2O.[25] This value and the above potential energy function were inserted into the periodic 1D torsional Schrödinger equation[37] and solved numerically. The resulting torsional levels are shown in Figure 4a for barrier heights ranging from 0 to 250 cm^{-1}. The optically allowed $\nu = 2^+ \leftarrow \nu = 0^+$ and the $\nu = 2^- \leftarrow \nu = 0^-$ torsional overtone transitions[26−28] are predicted to lie in the frequency range of 100−138 and 155−182 cm^{-1}, respectively, for barrier heights ranging from V_2 = 130 to 200 cm^{-1}.

When simultaneously fitting both the barrier height V_2 and the reduced rotational constant F_{red} to the experimental data (cf. section 3.7), we obtain an effective 1D barrier height of $V_2(S_1)$ = 213.4 cm^{-1} and a somewhat lower internal rotational constant F_{red} = 10.89 cm^{-1}. The latter value may be quite reasonable, since the reaction path for the torsional hydrogen exchange motion involves *not* simply a rigid-body rotation of the water molecule but also motions along the β_2 wag, the ρ_2 rock, and probably also the σ stretching coordinates. This combined multidimensional motion results in an increase of the mass-weighted torsional path length with respect to a purely rigid torsion around the C_2 axis of the water molecule. This in turn decreases the internal rotational constant F_{red} relative to that calculated simply by rigid rotation along τ.

The torsional levels resulting from the simultaneous fit of V_2 and F_{red} are shown in Figure 4b for barrier heights ranging from 0 to 250 cm^{-1}. For the ab initio barrier heights in the electronic ground-state which were calculated to lie in the range 233−240 cm^{-1} (see above) and an assumed barrier height $V_2(S_1)$ = 213 cm^{-1}, the torsional splitting of the electronic origin $0^{0^+}_{0^+}/0^{0^-}_{0^-}$ (i.e., between the $A_1' \leftarrow A_1''$ and $E' \leftarrow E''$ subbands) is calculated to be only 0.05 cm^{-1} for 6-HQ·H_2O. This splitting is too small to be observed at our laser resolution of ≈0.3 cm^{-1}. Compared to phenol·H_2O, for which Helm et al. determined a $0^{0^+}_{0^+}/0^{0^-}_{0^-}$ splitting of 0.8491 cm^{-1},[27] the torsional tunneling splitting of the electronic origin for 6-HQ·H_2O is predicted to be smaller by a factor of 16.

3. Experimental Results and Discussion

3.1. Experimental Procedure. The 6-HQ·H_2O complexes were synthesized and cooled in a pulsed supersonic expansion using neon carrier gas at 1.3 bar backing pressure. Neon carrier gas was flowed through a stainless steel reservoir containing H_2O at 273 K, giving an admixture of ≈0.5% water vapor. The mixture was flowed through the sample holder with 6-HQ (K&K Labs) and expanded through a magnetically actuated pulsed nozzle at 420 K. Typical nozzle opening times were 200 μs fwhm. Two-color resonant two-photon ionization (2C-R2PI) spectra were measured by crossing the jet with overlapping excitation and ionization laser beams inside the source of a linear time-of-flight mass spectrometer. For 6-HQ, the frequency doubled output (50 μJ/pulse) of a Lambda Physik dye laser pumped by the second harmonic of a Nd:YAG laser was used for excitation and the 266 nm fourth harmonic of the same Nd:YAG for ionization (4.5 mJ/pulse). For 6-HQ·H_2O, the excitation pulse energy was (200 μJ/pulse) and ionization was performed close to the ionization potential (IP) by a second frequency-doubled dye laser. The IP of 6-HQ·H_2O was measured to be 62 750 cm^{-1}. The ions were detected by a linear 1.0 m time-of-flight (TOF) mass spectrometer using double multichannel plates. The resulting mass spectra were digitized in a LeCroy 9350A 500 MHz digital oscilloscope, averaged over 50 shots and transferred to a PC.

For UV spectral hole-burning (HB) measurements, a third independently tunable frequency-doubled dye laser with a higher pulse energy (1.5 mJ/pulse) was used. It was pumped by a second Nd:YAG laser, which was fired 110 ns before the first Nd:YAG. Temporal synchronization between the lasers was maintained by a Stanford SRS 535 digital delay unit. The HB laser beam was spatially overlapped with the excitation and ionization laser beams.

For the dispersed fluorescence emission experiments an excitation energy of 0.5 mJ/pulse was used. The laser beam crossed the jet 5 mm downstream from the nozzle. The emitted fluorescence radiation was collected with a combination of a 60 mm diameter quartz lens (f = 150 mm) and a spherical mirror and dispersed in a 1.5 m Sopra UHRS-1500 monochromator with a curved entrance slit and a 2160 grooves/mm ruled grating, blazed at 500 nm. In first order, the reciprocal linear dispersion of this instrument is 2.3 Å/mm or ≈22 cm^{-1}/mm. The dispersed fluorescence was detected by a LN_2-cooled back-illuminated CCD chip with 1752 × 532 pixels of 15 μm^2 pixel size (Princeton Instruments CCD-1752PB/UVAR). Owing to the extremely weak fluorescence of the 6-HQ·H_2O complexes, long exposure times had to be used. Typically, two to four exposures

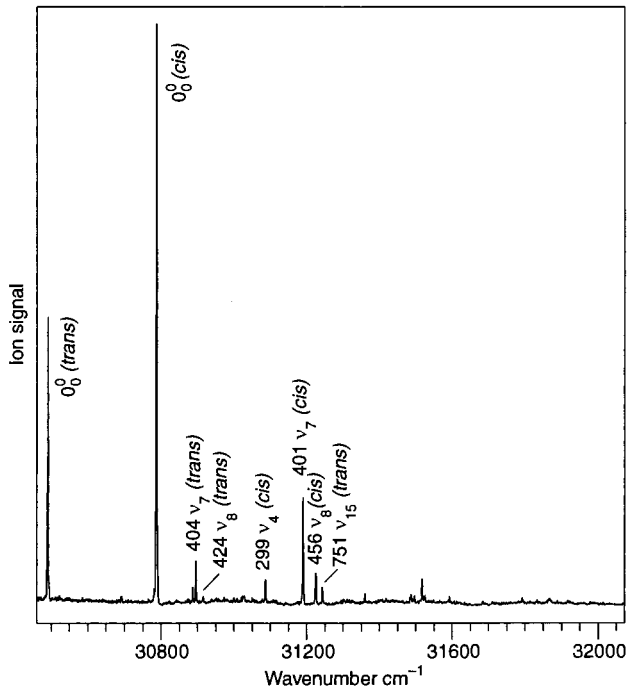

Figure 5. Two-color resonant two-photon ionization spectrum of 6-HQ over the range 30400−32000 cm^{-1}. Note the strong electronic origins of trans-6-HQ at 30491 cm^{-1} and cis-6-HQ at 30788 cm^{-1}. Vibronic bands due to one or the other rotamer were identified by UV laser hole-burning measurements.

TABLE 4: Experimental Intramolecular Vibrational Frequencies in the S_0 and S_1 States of *cis*- and *trans*-6-Hydroxyquinoline

assignment	freq. (cm^{-1}) *trans*-6HQ	freq. (cm^{-1}) *cis*-6HQ	assignment	freq. (cm^{-1}) *trans*-6HQ	freq. (cm^{-1}) *cis*-6HQ
		S_0 State[a]			
ν_4''		299	ν_{15}''	769	772
$2\nu_2''$		341	$2\nu_6''$	810	807
ν_7''	426	427	$2\nu_7''$	853	856
ν_8''	462	462	$\nu_7''+\nu_8''$		889
ν_{10}''	547	541	ν_{21}''	961	
$2\nu_5''$		573	$\nu_7''+\nu_{10}''$	970	964
ν_{12}''	618	618	$\nu_7''+\nu_{15}''$	1196	1198
$2\nu_3''$		624	$\nu_8''+\nu_{15}''$	1238	
ν_{14}'		728			
		S_1 State			
ν_4'		299	ν_8'	424	456
ν_7'	404	401	ν_{15}'	761	

[a] For a description of the normal modes, see ref 38.

of 15 min each were taken. The spectra were obtained by subtracting the background from the full frame image, correcting for the slit curvature, removal of spikes due to cosmic radiation, and binning of the corrected full frame image.

3.2. 6-Hydroxyquinoline. 2C-R2PI spectra of 6-hydroxyquinoline were taken over the range 30400−31400 cm^{-1} and are shown in Figure 5. The most intense bands of 6-HQ are at 30491 and 30788 cm^{-1}, separated by 297 cm^{-1}. Each of these bands give rise to an $S_1 \leftarrow S_0$ vibronic spectrum with similar vibrational structure, as reported in Table 4 with assignments based on the calculated harmonic frequencies obtained at the HF 6-31G(d,p) level.[38] A very similar situation prevails for 2-naphthol, for which two strong bands were found at 30586 and 30903 cm^{-1}, separated by 317 cm^{-1}.[12] These were shown to be due to the origins of the trans (or anti) and cis (or syn) rotamers, respectively, by detailed analysis of the resolved rotational structure of the origins. Johnson et al. showed that

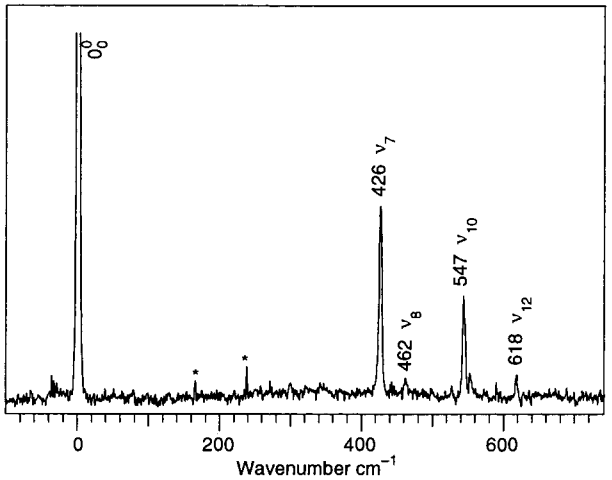

Figure 6. Dispersed fluorescence emission spectra of *trans*-6-HQ, excited at its electronic origin at 30491 cm^{-1}. Peaks marked by * are identified as spikes from cosmic radiation.

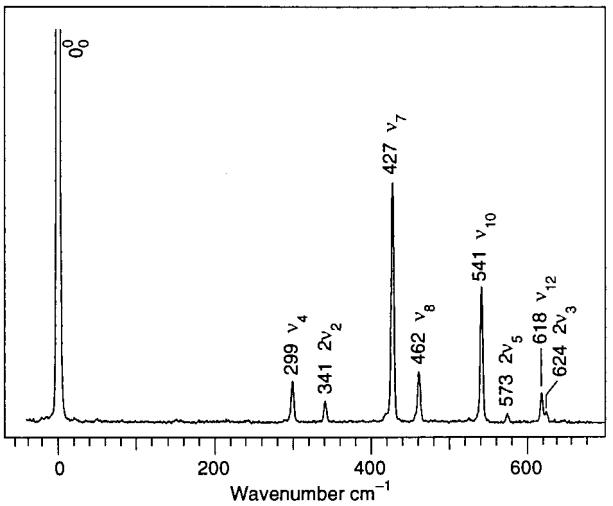

Figure 7. Dispersed fluorescence emission spectra of *cis*-6-HQ, excited at its electronic origin at 30788 cm^{-1}.

the origin at *lower* transition frequency must be assigned to the trans and the origin at higher frequency to the cis rotamer.[12] Since the relative intensities and the frequency difference of the two origins of 6-HQ are so similar to the closely analogous 2-naphthol, we assign by analogy the weaker lower-frequency band as due to the trans and the more intense origin at higher frequency to the cis rotamer of 6-HQ.

We note that the situation in the analogous 2-hydroxyquinoline molecule is very different: here there is a single electronic origin, which Held et al. determined to be the cis form by high-resolution UV laser spectroscopy.[22] The cis rotamer of 2-hydroxyquinoline is differentially stabilized by an intramolecular hydrogen bond to the neighboring nitrogen atom.

Figures 6 and 7 show the dispersed fluorescence emission spectra of 6-HQ obtained by exciting at the 0_0^0 band of trans-6-HQ rotamer at 30491 and at the 0_0^0 band of the cis-6-HQ at 30788 cm^{-1}, respectively. Here, we show only the low-frequency ranges, which are relevant for the later analysis of the intermolecular vibrations of the *trans*- and *cis*-6-HQ·H_2O complexes.

The observed S_0 state vibrational frequencies and the Franck−Condon distributions are generally similar, but slightly different in detail, confirming the assumption that they correspond to ground-state species of similar structure. The main vibrational

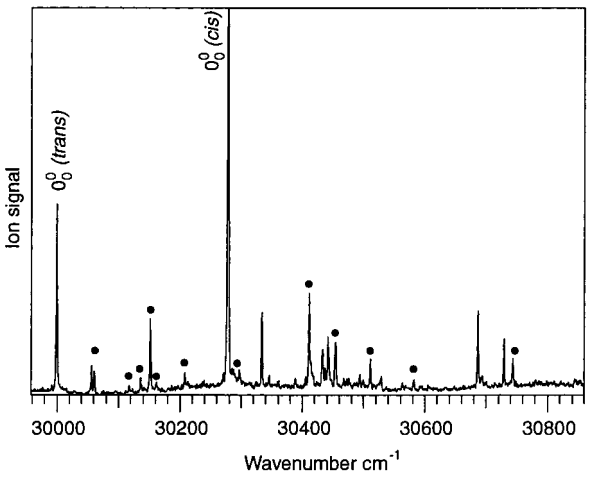

Figure 8. 2C-R2PI spectrum of *cis*- and *trans*-6-hydroxyquinoline·H_2O complexes over the range 29960−30860 cm^{-1}. The electronic origins at 29 998 and 30 277 cm^{-1} are assigned to the trans and cis rotamers, respectively. The red shifts are 493 cm^{-1} (trans) and 510 cm^{-1} (cis). All bands marked by • were identified as due to the trans rotamer by spectral hole-burning measurements (see text).

modes are at ≈426, 462, 544, and 618 cm^{-1}. For the cis rotamer, we detect additional vibrations at 299, 341, 573, and 624 cm^{-1}. These are skeletal deformation modes of the quinoline ring system; the detailed assignments will be discussed elsewhere.[38]

Fluorescence Lifetime and Quantum Yield. The fluorescence lifetime of bare *cis*-6-hydroxyquinoline was measured as $\tau_{fl} = 5 \pm 1$ ns. This is much shorter than the fluorescence lifetime observed for jet-cooled 1-naphthol, which has $\tau_{fl} = 61 \pm 2$ ns.[15] For 1-HN the fluorescence lifetime is very close to the radiative lifetime, and hence its fluorescence quantum yield is $\phi_{fl} \approx 1$. Assuming that the $S_1 \leftarrow S_0$ oscillator strengths of structurally and electronically very similar 1-HN and 6-HQ molecules are the same, we can estimate the fluorescence quantum yield of 6-HQ as $\phi_{fl} \approx 0.1$.

Complexation with one molecule of water reduced the observed τ_{fl} to approximately the 4−5 ns temporal pulse width of the excitation laser, which implies a fluorescence lifetime <1 ns, and a concurrent reduction of the fluorescence quantum yield to $\phi_{fl} < 0.015$.

3.3. 6-Hydroxyquinoline·H_2O Complex. An overview 2C-R2PI spectrum of the 6-HQ·H_2O complex is presented in Figure 8. The two most intense bands in the spectrum at 29 998 and 30 277 cm^{-1} are assigned as the electronic origins of the trans and cis rotamer, respectively. This is based first on the analogous assignments for 2-HN[12] and second on the assumption that the origins of both rotamers are shifted by similar amounts upon complexation with H_2O, as was earlier assumed for 2-naphthol·H_2O.[25] This assumption is also supported by the relative intensities of the electronic origins of 6-HQ·H_2O, since the trans origin is weaker and the cis origin band at higher frequency is more intense, in approximately the same 1:2 cis:trans ratio as for the bare 6-HQ rotamers.

With these assignments, the spectral red shifts due to complexation with water amount to $\delta\nu = -493$ cm^{-1} (1.41 kcal/mol) for the trans and $\delta\nu = -510$ cm^{-1} (1.46 kcal/mol) for the cis rotamer. These values represent the *increases* of hydrogen-bond dissociation energy upon electronic excitation. They are ≈150 cm^{-1} (0.4 kcal/mol) larger than for 2-naphthol·H_2O.[25]

The R2PI spectra of the two rotameric species were then separated by UV spectral hole-burning. The bands of the trans-rotamer are marked by a • in Figure 8. The R2PI spectrum of

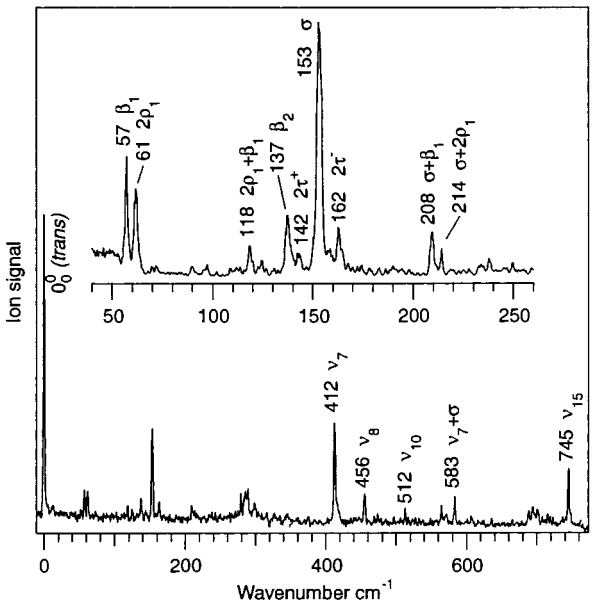

Figure 9. Two-color resonant two-photon ionization spectrum of pure *trans*-6-HQ·H_2O. A second UV laser is operated at the cis rotamer 0_0^0 band at 30 277 cm^{-1}, to remove all signals due to this rotamer to <1%. The insets show magnified spectra of the intermolecular vibrational frequency ranges.

TABLE 5: Experimental Intermolecular Vibrational Frequencies and Relative Intensities in the S_0 and S_1 Spectra of *cis*- and *trans*-6-HQ·H_2O

assignment	freq. (cm^{-1})	rel. int. (%)	assignment	freq. (cm^{-1})	rel. int. (%)
		S_0 (0_0^0 excitation)			
		trans-6-HQ·H_2O			
β_1''	54	5.1	β_2''	161	6.4
σ''	140	6.5			
		cis-6-HQ·H_2O			
β_1''	47	3.3	$3\beta_1''$	152	1.7
$2\rho_1''$	57	1.6	β_2''	161	2.5
σ''	141	4.2			
		S_1			
		trans-6-HQ·H_2O			
β_1'	57	12.6	σ'	153	27.0
$2\rho_1'$	61	7.8	$2\tau'^-$	162	5.0
$\beta_1' + 2\rho_1'$	118	3.0	$\sigma' + \beta_1'$	208	4.4
β_2'	137	6.0	$\sigma' + 2\rho_1'$	214	2.6
$2\tau'^+$	142	1.5			
		S_1			
		cis-6-HQ·H_2O			
β_1'	56	9.6	$2\tau'^-$	159	2.6
$2\rho_1'$	68	1.3	σ'	164	9.3
$2\beta_1'$	111	1.0	$3\beta_1'$	166	5.0
β_2'	155	6.0	$\sigma' + \beta_1'$	210	1.3

pure trans-6-HQ·H_2O, which was separated by hole-burning, is shown in Figure 9. For this spectrum the hole-burning laser was tuned to the 0_0^0 of the cis rotamer at 30 277 cm^{-1}; the bands associated with the cis rotamer were reduced to less than 1% of their original intensity. Intramolecular bands of *trans*-6-HQ·H_2O appear at 0_0^0(trans) +412, +456, +512, +533, and +745 cm^{-1}. Intermolecular bands with weaker intensity are observed in the range up to 250 cm^{-1} of the origin. Frequencies and intensities relative to the 0_0^0 band are given in Table 5.

R2PI spectra of pure cis-6-HQ·H_2O are shown in Figure 10. To obtain these, the hole-burning laser was tuned to the trans rotamer origin at 29 998 cm^{-1}, again resulting in almost complete removal of the bands of this species to <1% of the original intensity. Intramolecular bands appear at 0_0^0 (cis)

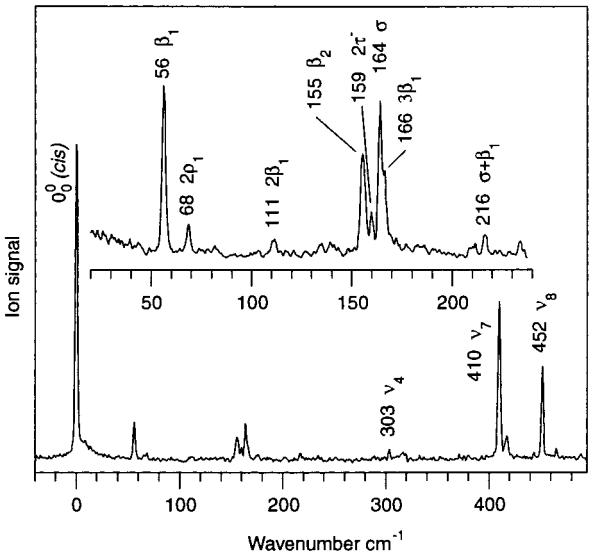

Figure 10. Two-color resonant two-photon ionization spectrum of pure *cis*-6-HQ·H_2O complex. A second UV laser is operated at the trans rotamer 0_0^0 band at 29 998 cm^{-1}, to remove all signals due to the other rotamer to <1%. The insets show magnified spectra of the intermolecular vibrational frequency ranges.

+303, +410, and +452 cm^{-1}. Again, the intermolecular bands in the range up to +250 cm^{-1} are weaker, but they are clearly apparent in the inset spectrum. The most prominent transitions lie at +56 cm^{-1} and between 150 and 170 cm^{-1}. Frequencies and intensities relative to the 0_0^0 band are given in Table 5.

The dispersed fluorescence emission spectra obtained by exciting the electronic origin of the trans-6-HQ·H_2O complex are shown in Figure 11a. This yields three weak intermolecular bands at +54, +140, and +161 cm^{-1}. By exciting the 0_0^0 band of the cis-6-HQ·H_2O complex, five weak intermolecular bands appear in the spectra at +47, +57, +141, +152, and +161 cm^{-1}, which are shown in Figure 11b. Identified intramolecular bands are at 0_0^0 +442, +428, +556 cm^{-1} (trans) and +311, +340, +432, +467 cm^{-1} (cis). Frequencies and intensities relative to the 0_0^0 band are given in Table 5.

3.4. Stretching Vibrations. In analogy to 2-naphthol·H_2O (ref 25), we assign the most intense intermolecular band at +153 cm^{-1} in the R2PI spectra of the trans-6-HQ·H_2O complex to the S_1 state intermolecular stretching mode σ' of the trans rotamer. In the related 2-HN·H_2O complex, the σ' fundamental is 147 cm^{-1},[25] which is 6 cm^{-1} or 4% lower.

For the cis rotamer, the situation is more complicated: in the R2PI spectrum, one observes a group of four bands at +155, +159, +164, and +166 cm^{-1}, and these may be coupled by Fermi resonance interactions. The strongest of these lies at 164 cm^{-1}; since the transition moment of this group of bands derives mainly from the stretching transition, we assign this as being dominantly the "stretch" σ' state. In the related *cis*-2-HN·H_2O complex, the σ' fundamental lies at 154 cm^{-1};[25] this is 7 cm^{-1} or 5% higher than the 147 cm^{-1} σ' fundamental of the trans 2-HN·H_2O (see above). If a similar relation holds also for *trans*- and *cis*-6-HQ·H_2O, then the predicted stretching fundamental for the cis rotamer is at ≈160 cm^{-1}.

The σ'' S_0 ground-state intermolecular stretching fundamental is assigned as the band observed at 140 cm^{-1} in the emission spectra of *trans*-6-HQ·H_2O.

In the emission spectra of *cis*-6-HQ·H_2O, we observe a group of bands at +141, +152, and +161 cm^{-1}, roughly similar to the group of bands in the R2PI spectrum. We assign the +141 band to a state that carries predominantly σ'' stretching character,

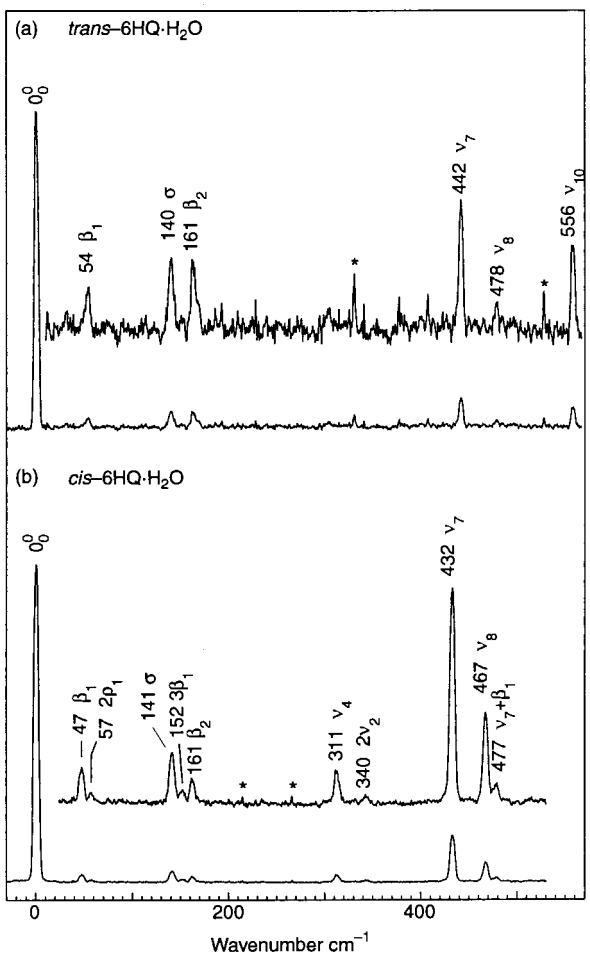

Figure 11. Dispersed fluorescence emission spectra of (a) *trans*-6-HQ·H_2O, excited at the trans electronic origin at 29 998 cm^{-1}; (b) *cis*-6-HQ·H_2O, excited at the cis rotamer origin at 30 277 cm^{-1}. Peaks marked by * are identified as spikes from cosmic radiation.

based on its highest intensity. This assignment implies that the cis intermolecular stretching frequency $\nu_{\sigma''}$ is slightly higher than that for *trans*-6-HQ·H_2O. This is in agreement with (i) the assignments for the S_1 state (see above), (ii) the situation found previously for 2-naphthol·H_2O,[25] and (iii) the ab initio calculations of section 2. There, the harmonic intermolecular σ'' frequencies for *cis*- and *trans*-6-HQ·H_2O were calculated as 153 and 148 cm^{-1}, respectively (see Tables 2 and 3). Anharmonicity is expected to lower the calculated frequencies.

3.5. Wagging Vibrations. In C_s symmetry, only the a' (in-plane) modes should couple strongly with the $S_1 \leftrightarrow S_0$ electronic transitions. Thus the intermolecular wagging modes β_1 and β_2 of a' symmetry are expected to appear in the spectra. In the emission spectra of both the trans and cis rotamers, see Figure 11, the low-frequency β_1'' wag fundamentals can be clearly identified as the bands at +54 cm^{-1} (*trans*-6-HQ·H_2O) and at +47 cm^{-1} for *cis*-6-HQ·H_2O. The calculated harmonic frequencies agree very well, being 56 and 50 cm^{-1}, respectively, i.e., 2 and 3 cm^{-1} higher than observed for both species. The calculation predicts that the trans $\nu_{\beta_1''}$ frequency is 12% higher than for the cis rotamer, in excellent agreement with observation. We point out that this is just the opposite found for the intermolecular stretching vibrations.

In the R2PI spectra of *trans*-6-HQ·H_2O, the second strongest intermolecular band at +57 cm^{-1} probably corresponds to the β_1' state. There is a close-by transition at 61 cm^{-1}, probably due to the rock overtone (see below). For the cis rotamer, the

β_1' mode is quite intense, with a relatively strong isolated band at +56 cm^{-1}, and continuing as a short progression with further members at +111 cm^{-1} and probably +166 cm^{-1}. The latter transition is a band on the blue side of the intermolecular σ' stretch.

In phenol·H_2O (ref 26) (121 cm^{-1}) and 2-naphthol·H_2O,[25] the β_2'' and β_2' high-frequency wagging fundamentals are known to lie close to the intermolecular stretching fundamentals and couple strongly by Fermi resonance. Here we find a similar situation: Addressing first the emission spectra, for the trans rotamer we assign the band at +161 cm^{-1} as the β_2'' fundamental. We note that it is just as intense as the band assigned to the σ'' fundamental, and the two states are probably strongly mixed. For the cis rotamer in the S_0 state, there is a group of at least three bands at +141/+152/+161 cm^{-1}. The second strongest band at 161 cm^{-1} is tentatively assigned as being dominantly β_2'', in keeping with the trans rotamer. The weakest middle band may be due to $3\beta_1''$, enhanced by Fermi resonance with both the σ'' and β_2'' states.

In the R2PI spectra, β_2 cannot be assigned unequivocally. For the cis rotamer the β_2' fundamental must be contained in the group of four bands at +155/+159/+164/+166 cm^{-1}. It is tentatively assigned as the second strongest and lowest-frequency band in this group at 155 cm^{-1}. For the trans rotamer, there are two likely candidates, at 137 and 162 cm^{-1}. Since there is a reasonable assignment for the latter band as a torsional overtone (see below), we assign the 137 cm^{-1} band as the trans β_2' fundamental. For β_2'' the ab initio calculated and experimental frequencies do not agree as well as for β_1 or σ. In the harmonic approximation the β_2 ground-state frequencies are overestimated by 40%−50% for both cis and trans. As was previously pointed out for phenol·H_2O (ref 26) and 2-naphthol·H_2O,[25] the β_2 vibration suffers from a poor description in the harmonic approximation: the wagging mode is essentially a hindered rotation of the water molecule, showing large-amplitude excursions of the hydrogen atoms and low reduced mass. Presumably, the intermolecular potential along β_2 is also strongly anharmonic for 6-HQ·H_2O, leading to a large frequency decrease.

3.6. Rocking Vibrations. Both of the rocking mode fundamentals ρ_1 and ρ_2 are a'' and hence symmetry-forbidden within the $S_1 \leftrightarrow S_0$ transition. In first order they are only expected as sequences, overtones, or combinations. However, the large amplitude motions associated with the intermolecular vibrations may give rise to Herzberg−Teller-type effects, which may lead to observably intense a″ fundamentals in the spectra. The calculated S_0 state ρ_1 harmonic fundamental frequencies for trans and cis rotamers are 26 and 31 cm^{-1}, respectively; for the high-frequency ρ_2 rocking modes they are 218 and 232 cm^{-1}, respectively; cf. Tables 2 and 3.

The strongest evidence for intermolecular rocking transitions are the bands at +61 and +68 cm^{-1} in the R2PI spectra of the trans and cis rotamers. Both bands are attributed to the $2\rho_1'$ gaining in intensity by Fermi resonances with the β_1 mode. For the trans rotamer, the frequencies are closer, with the β_1 and $2\rho_1'$ at 57 and 61 cm^{-1}, and hence a larger gain in intensity is observed than for the cis rotamer, where the putative $2\rho_1'$ state lies 12 cm^{-1} above the β_1 transition. A weak band, which may be due to the $2\rho_1'$ state, appears at 57 cm^{-1} in the emission spectrum of the cis rotamer, with an intensity ratio relative to the β_1'' state, which is quite similar to that of the R2PI spectrum. The trans rotamer emission spectrum shows no clear sign of a $2\rho_1'$ state, although the β_1'' band seems broadened to the red.

TABLE 6: Comparison of Experimental Intermolecular Frequencies in the S_0 and S_1 States of the Hydrogen-Bonded 6-Hydroxyquinoline·H_2O, 2-Naphthol·H_2O, 1-Naphthol·H_2O, and Phenol·H_2O Complexes

	trans-6-HQ[a]	*cis*-6-HQ[a]	*trans*-2-HN[b]	*cis*-2-HN[b]	1-HN[c]	phenol
			S_0 State			
ρ_1''[d]		28.5		27.5		
β_1''	54	47	54	47		57[e]
σ''	140	141	141	153		155[e]
β_2''	161	161	166	141		146[e]
			S_1 State			
ρ_1'[d]	30.5	34	26.5	32		29.7[f]
β_1'	57	56	59	55	57	66.9[f]
σ'	153	164	147	154		156[f]
β_2'	137	155	130	132		120.5/125.9[f]

[a] This work. [b] Reference 25. [c] Reference 31. [d] One-half of the overtone frequency. [e] References 25, 29. [f] References 27, 28.

Experimental ρ_1 and computed (harmonic) overtone frequencies agree within ≈5%. There is no evidence for ρ_2 overtone or combination bands, either in absorption or in emission.

3.7. Torsional Vibrations. According to the selection rules of the torsional mode discussed in refs 25 and 26 only transitions with $\Delta\nu = 0, \pm 2, \ldots$ are allowed for τ within the $S_1 \leftrightarrow S_0$ electronic transition. For barrier heights of 130−100 cm^{-1}, the $\nu = 2^+ \leftarrow \nu = 0^+$ and the $\nu = 2^- \leftarrow \nu = 0^-$ transitions are predicted to lie in the frequency range of 100−138 and 155−182 cm^{-1}, respectively (cf. section 2.5). In the R2PI spectrum of the trans rotamer, two weak features appear at 142 and 162 cm^{-1}, which we tentatively assign to the $\nu = 2^+ \leftarrow \nu = 0^+$ and $\nu = 2^- \leftarrow \nu = 0^-$ transition of τ'. For the cis rotamer the $\nu = 2^- \leftarrow \nu = 0^-$ transition will be contained in the group of four bands at +155/+159/+164/+166 cm^{-1}. According to the assignment of the bands given above the band at 159 cm^{-1} is assigned to this transition. As described in section 2.5, we obtain a effective 1D barrier height of $V_2 = 213$ cm^{-1} for the S_1 state with this assignment. No indications for transitions in τ are evident from the dispersed fluorescence emission spectra.

4. Comparison of Intermolecular Frequencies for the Complexes of 6-Hydroxyquinoline, 1- and 2-Naphthol, and Phenol with Water

The present study of hydrogen bonding and vibrations of the 6-HQ·H_2O complex complements earlier combined experimental and theoretical work of the related 2-naphthol·H_2O,[25] 1-naphthol·H_2O,[31] and phenol·H_2O[26−30,33,34] complexes. In this section, we compare the intermolecular vibrational frequencies in the S_0 and S_1 state, which characterize the O−H···O hydrogen bonds of these complexes.

The intermolecular vibrational frequencies of the a′ H-bond stretch σ, the two a′ wags β_1, β_2, and the a″ rock ρ_1 in both the S_0 and S_1 state for these complexes are collected in Table 6.

Addressing first the ρ_1 rock mode, which in this work was observed experimentally as the first overtone of the fundamental gaining in intensity by Fermi resonance with the β_1 mode, we note that for 6-HQ the cis ρ_1' frequency is *higher* than that of the trans. The same situation is also observed for ρ_1' frequencies of the 2-naphthol·H_2O rotamers.

Comparing the hydrogen-bond stretching mode σ, for both the S_0 and S_1 states of both 6-HQ and 2-naphthol, the σ frequency of the cis rotamer is always 6−8% higher in frequency than the trans. This is the same behavior as for the ρ_1 low-frequency rock.

The opposite is observed for the β_1 wag: In both the S_0 and S_1 electronic states of both 6-hydroxyquinoline·H_2O and

2-naphthol·H_2O the β_1'' and β_1' frequencies are higher for the trans rotamer. For the structurally and electronically very similar 1-naphthol·H_2O, only the S_1 state β_1' mode was observed by Knochenmuss et al.[31]

For the high-frequency β_2 wag, significant differences are found among the complexes and rotamers compared in this section. For 6-HQ·H_2O, as also for 2-naphthol·H_2O, the β_2 fundamental states lie close to the intermolecular σ stretch fundamentals and are strongly coupled to these by Fermi resonance. We have adopted the convention that the more intense band is assigned to the σ transition, the weaker to the β_2 transition.

The agreement of the β_2'' frequencies with the ab initio harmonic frequency calculations is generally poor. For phenol·H_2O, Schütz et al.[26] have pointed out that β_2'' is poorly described in the harmonic approximation. It is essentially a hindered rotation of the water molecule with large-amplitude excursion of the hydrogen atoms and low reduced mass; the corresponding intermolecular potential is strongly asymmetric, leading to large anharmonic corrections.[26] The same is true for 2-naphthol·H_2O.[25] For the S_1 state phenol·H_2O complex, Schmitt et al.[28] and Helm et al.[27] have recently proposed that β_2' exhibits two torsional subbands with a large torsional splitting of -4.59 cm^{-1}, indicating a strong coupling of the high-frequency wagging vibration and the torsional motion. We point out that for *trans*-6HQ·H_2O, *cis*-6HQ·H_2O, and *trans*-2-HN·H_2O, the β_2'' fundamentals are $\approx$20 cm^{-1} higher than the σ'' fundamentals. For cis-6HQ·H_2O and phenol·H_2O, the $\sigma'' \leftrightarrow \beta_2''$ coupling in the electronic ground state is stronger and the identification of the states as "σ''" or "β_2''" is problematic. Thus the seeming reversal of σ and β_2 frequency apparent from Table 6 for these two complexes reflects the difficulty of giving a unique assignment.

Compared to the phenol complex, the 6-HQ and 2-naphthol ρ_1 and β_1 are very close in relative frequency.

Finally, comparing the S_0 and S_1 state intermolecular vibrational frequencies for the modes and aromatic molecules discussed in this section, we note that for all modes except β_2 the S_1 state frequencies increase by 5−20%, while for the β_2 wags, electronic excitation leads to a 10−20% decrease.

5. Conclusions

In this study we extended our investigation to 6-HQ·H_2O. Geometry optimization at the SCF 6-31G(d,p) level yield trans-linear hydrogen bonding arrangements with C_s symmetry as minimum-energy structures for both the cis and trans rotamers, similar to the 2-naphthol·H_2O reported previously. Small deviations in the structural parameters occur between the *cis*- and *trans*-6-HQ·H_2O and between 6-HQ·H_2O and 2-naphthol·H_2O, calculated at the same level of theory. However, the hydrogen-bond distance R(O...O) shows a continuous shortening along the series phenol, *trans*-2-naphthol, *cis*-2-naphthol, *trans*-6-hydroxyquinoline to *cis*-6-hydroxyquinoline. The transition structures of *cis/trans*-6-HQ·H_2O on the H_2O hydrogen atom exchange pathway were also explored by full optimization to first-order saddle points on the related HF 6-31G(d,p) PES. As for phenol·H_2O and 2-naphthol·H_2O, nonplanar C_1 structures were obtained with the H_2O oxygen atom 0.35 Å above the ring plane. The barrier heights to internal rotation amount to 233 and 240 cm^{-1} for the trans and the cis rotamer in the electronic ground state, again very similar to the corresponding 2-naphthol·H_2O value. Furthermore, harmonic vibrational analysis using analytical second derivatives of the HF 6-31G(d,p) PES was carried out for the *cis/trans*-6-HQ·H_2O minimum-energy structures with main focus on the six intermolecular modes, characterized as an a′ H-bond stretch σ, an a″ H-bond torsion τ, two a′ wags β_1, β_2, and two a″ rocks ρ_1, ρ_2 in the C_s symmetry group. The anharmonic vibrational levels for τ (H_2O hydrogen atom exchange coordinate) were computed using a 1D $V = V_2(1 - \cos 2\phi)/2$ periodic potential, and the estimated barrier heights for internal hindered rotation are 213 cm^{-1} in the S_1 state.

On the experimental side, $S_1 \leftarrow S_0$ vibronic spectra were measured using 2C-R2PI spectroscopy. The vibronic bands belonging to the cis and trans rotamers were unequivocally identified and separated via UV laser spectral hole-burning. Following identification of both cis and trans electronic origins, dispersed $S_1 \rightarrow S_0$ fluorescence emission spectra were measured. Complexation of the parent 6-HQ molecule decreases the observed fluorescence lifetime from $\tau_{fl} = 5$ ns to <1 ns, and the estimated fluorescence quantum yield from $\phi_{fl} \approx 0.1$ to <0.015. Despite this low quantum yield, intermolecular vibrational transitions for the low- and high-frequency bending vibrations β_1 and β_2 and the intermolecular stretching mode σ of both cis and trans rotamers were measured for both the S_1 and S_0 states. In all cases except the trans rotamer S_0 state, the $2\rho_1$ overtones of the low-frequency rocking mode were observed via Fermi resonances with the β_1 states. The assignments of the ground-state levels were based on the calculated intermolecular frequencies and are generally are in good agreement, except for the β_2'' bending mode.

Acknowledgment. This work was supported by the Schweiz. Nationalfonds (projects 20-40669.94 and 20-47214.96).

References and Notes

(1) Mason, S. F.; Philip, J.; Smith, B. E. *J. Chem. Soc. A* **1968**, 3051.
(2) Schulman, S. *Anal. Chem.* **1971**, *43*, 285.
(3) Bardez, E.; Chatelain, A.; Larrey, B.; Valeur, B. *J. Phys. Chem.* **1994**, *98*, 2357.
(4) Schulman, S.; Fernando, Q. *Tetrahedron* **1968**, *24*, 1777.
(5) Lavin, A.; Collins, S. *Chem. Phys. Lett.* **1993**, *204*, 96.
(6) Bohra, A.; Lavin, A.; Collins, S. *J. Phys. Chem.* **1994**, *98*, 11424.
(7) Thistlethwaite, P.; Corkill, P. *Chem. Phys. Lett.* **1982**, *85*, 317.
(8) Thistlethwaite, P. *Chem. Phys. Lett.* **1983**, *96*, 509.
(9) Tokumura, K.; Itoh, M. *J. Phys. Chem.* **1984**, *88*, 3921.
(10) Itoh, M.; Adachi, T.; Tokumura, K. *J. Am. Chem. Soc.* **1984**, *106*, 850.
(11) Lahmani, F.; Douhal, A.; Breheret, E.; Zehnacker-Rentien, A. *Chem. Phys. Lett.* **1994**, *220*, 235.
(12) Johnson, J.; Jordan, K.; Plusquellic, D.; Pratt, D. *J. Chem. Phys.* **1990**, *93*, 2258.
(13) Cheshnovsky, O.; Leutwyler, S. *Chem. Phys. Lett.* **1985**, *121*, 1.
(14) Cheshnovsky, O.; Leutwyler, S. *J. Chem. Phys.* **1988**, *88*, 4127.
(15) Knochenmuss, R.; Leutwyler, S. *J. Chem. Phys.* **1989**, *91*, 1268.
(16) Droz, T.; Knochenmuss, R.; Leutwyler, S. *J. Chem. Phys.* **1990**, *93*, 4520.
(17) Steadman, J.; Syage, J. A. *J. Chem. Phys.* **1990**, *92*, 4630.
(18) Syage, J. A. *J. Phys. Chem.* **1993**, *97*, 12523.
(19) Hineman, M. F.; Brucker, G. A.; Kelley, D. F.; Bernstein, E. R. *J. Chem. Phys.* **1992**, *97*, 3341.
(20) Kim, S.; Wang, J.; Zewail, A. *Chem. Phys. Lett.* **1994**, *228*, 369.
(21) Nimlos, M. R.; Kelley, D. F.; Bernstein, E. R. *J. Phys. Chem* **1989**, *93*, 643.
(22) Held, A.;; Pratt, D. *J. Am. Chem. Soc.* **1993**, *115*, 9708.
(23) Mengel, M.; Leutwyler, S. Submitted to *J. Chem. Phys.*
(24) Mengel, M.; Leutwyler, S. Submitted to *J. Chem. Phys.*
(25) Schütz, M.; Bürgi, T.; Leutwyler, S.; Fischer, T. *J. Chem. Phys.* **1993**, *99*, 1469.
(26) Schütz, M.; Bürgi, T.; Leutwyler, S.; Fischer, T. *J. Chem. Phys.* **1993**, *98*, 3763.
(27) Helm, R.; Vogel, H.; Neusser, H. *J. Chem. Phys.* **1998**, *108*, 4496.
(28) Schmitt, M.; Jacoby, C.; Kleinermanns, K. *J. Chem. Phys.* **1998**, *108*, 4486.
(29) Stanley, R.; Castleman, A. *J. Chem. Phys.* **1991**, *94*, 7744.
(30) Stanley, R.; Castleman, A. *J. Chem. Phys.* **1993**, *98*, 796.
(31) Knochenmuss, R.; Karbach, V.; Wickleder, C.; Graf, S.; Leutwyler, S. *J. Phys. Chem. A* **1998**, *102*, 1935.

(32) Frisch, M. J.; Trucks, G. W.; Schlegel, H. B.; Gill, P. M. W.; Johnson, B. G.; Robb, M. A.; Cheeseman, J. R.; Keith, T.; Petersson, G. A.; Montgomery, J. A.; Raghavachari, K.; Al-Laham, M. A.; Zakrzewski, V. G.; Ortiz, J. V.; Foresman, J. B.; Cioslowski, J.; Stefanov, B. B.; Nanayakkara, A.; Challacombe, M.; Peng, C. Y.; Ayala, P. Y.; Chen, W.; Wong, M. W.; Andres, J. L.; Replogle, E. S.; Gomperts, R.; Martin, R. L.; Fox, D. J.; Binkley, J. S.; Defrees, D. J.; Baker, J.; Stewart, J. P.; Head-Gordon, M.; Gonzalez, C.; Pople, J. A. *Gaussian 94, Revision D.4;* Gaussian, Inc.: Pittsburgh, PA, 1995.

(33) Berden, G.; Meerts, W.; Schmitt, M.; Kleinermanns, K. *J. Chem. Phys.* **1996**, *104*, 972.

(34) Gerhards, M.; Schmitt, M.; Kleinermanns, K.; Stahl, W. *J. Chem. Phys.* **1996**, *104*, 967.

(35) Feller, D.; Feyereisen, M. W. *J. Comput. Chem.* **1992**, *14*, 1027.

(36) Bürgi, T.; Droz, T.; Leutwyler, S. *Chem. Phys. Lett.* **1995**, *246*, 291.

(37) Kroto, H. *Molecular Rotation Spectra;* Wiley: New York, 1972.

(38) Bach, A.; Hewel, J.; Leutwyler, S. To be published.